IEEE Access
Multidisciplinary ⋮ Rapid Review ⋮ Open Access Journal

Received May 28, 2019, accepted June 16, 2019, date of publication June 24, 2019, date of current version July 15, 2019.

Digital Object Identifier 10.1109/ACCESS.2019.2924494

Dual-Polarized Band-Notched Antenna Without Extra Circuit for 2.4/5 GHz WLAN Applications

YAOHUI ZHANG[1,3], YONGHONG ZHANG[1], DAOTONG LI[2,3], (Member, IEEE), KUNNING LIU[1], AND YONG FAN[1]

[1]School of Electronic Science and Engineering, University of Electronic Science and Technology of China (UESTC), Chengdu 611731, China
[2]Center of Aerocraft TT&C and Communication, Chongqing University, Chongqing 400044, China
[3]State Key Laboratory of Millimeter Waves, Nanjing 210096, China

Corresponding author: Daotong Li (dli@cqu.edu.cn)

This work was supported in part by the National Natural Science Foundation of China under Grant 61801059, in part by the Opening Subject of State Key Laboratory of Millimeter Waves under Grant K202016, in part by the Chongqing Special Found of Technology R&D for Academician under Grant cstc2018zdcy-yszxX0001, and in part by the Venture and Innovation Support Program for Chongqing Overseas Returnees under Grant cx2017095.

ABSTRACT In this paper, a dual-band dual-polarized crossed dipole antenna with good anti-interference capability is proposed for 2.4-/5-GHz WLAN applications. The proposed antenna covers the WLAN 2.4-GHz band (2.4–2.48 GHz) and 5-GHz bands (5.15–5.85 GHz) with isolation >27 dB for VSWR < 2. Without extra filtering circuit, a band-notch (3.4–3.6 GHz) is achieved by introducing the C-shaped split ring resonator (SRR) into the wideband dipole antenna. Compared with the original wideband dipole antenna, the minimum gain in the notched band is suppressed from 8 to −9 dBi and the gain in the higher band is improved from 6 to 9.7 dBi. The proposed antenna can realize a high gain of 7.85 dBi for the lower band and 9.7 dBi for the higher band. As demonstrations, two reference antennas and the proposed antennas are fabricated and measured, and the measured results agree well with the simulated ones.

INDEX TERMS Dual-band, dual-polarized, filtering antenna, band-notch, split ring resonator, high gain.

I. INTRODUCTION

With the rapid development of wireless communication systems, such as the base station [1] and WLAN applications [2]–[5], dual-band dual-polarized (DBDP) antennas working in two or multiple bands are necessary to alleviate the multipath fading and improve the channel capacity. In the MIMO WLAN applications, dual-band (2.4-2.484 and 5.15-5.85 GHz) dual-polarized antenna elements with high isolation and high gain are essential to achieve the desired wireless performance, especially for the high-density enterprise environments [5]. To avoid the interference from other bands, the configurable filtering antennas can achieve excellent performance for the 2.4/5 GHz WLAN applications [6], [7]. However, the extra active circuits make the antenna design complicated for most applications. The band-notch between two working bands is an effective way to suppress the interference from some other narrowband systems, such as the WiMAX and 5G communication systems (3.4-3.6 GHz).

Suitable band-notched suppression can be realized by dual-band antenna with sharp cut-off [8], [9] or wideband antenna with deep band-notch [10]–[13]. Although the dual-band antennas can realize band-notched suppression performance, wideband antennas with deep band-notch are more convenient to control the bandwidths of two bands and achieve similar characteristics for two bands. The microstrip antenna [10] can achieve a good band-notch by introducing a pair of crossed slots, four shorting pins and four parasitic strips. Nevertheless, the bandwidth of the antenna is not wide enough to cover 2.4/5 GHz WLAN applications. The Vivaldi antenna [11] with wide bandwidth can be utilized to achieve DBDP characteristic by using band-notched feeding line. However, the profile of the Vivaldi antenna is high and the gain is relatively low.

Because the crossed dipole antennas have the advantages of wide bandwidth, stable radiation patterns, compact size and ease of fabrication, they are widely used in wireless communication systems [12]–[13]. The filtering stubs near the feeding lines are introduced into the crossed dipole antenna to suppress the mutual coupling between the lower band and upper band [12]. Extra feeding balun circuits with C-shaped

The associate editor coordinating the review of this manuscript and approving it for publication was Lu Guo.

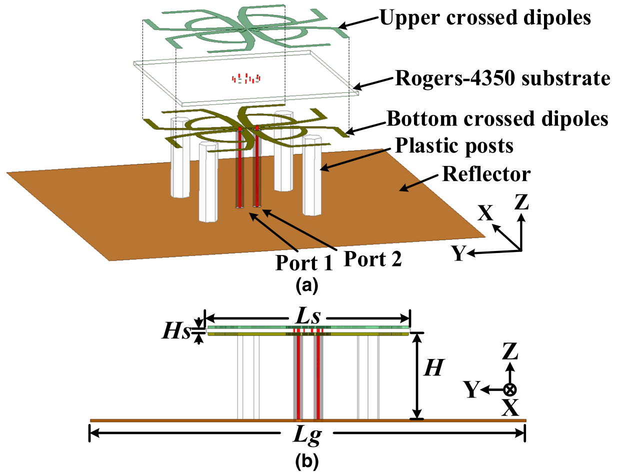

FIGURE 1. Structure of the proposed antenna. (a) 3-D view. (b) Side view. ($H = 16$ mm, $Hs = 0.787$ mm, $Lg = 80$ mm, $Ls = 37.5$ mm).

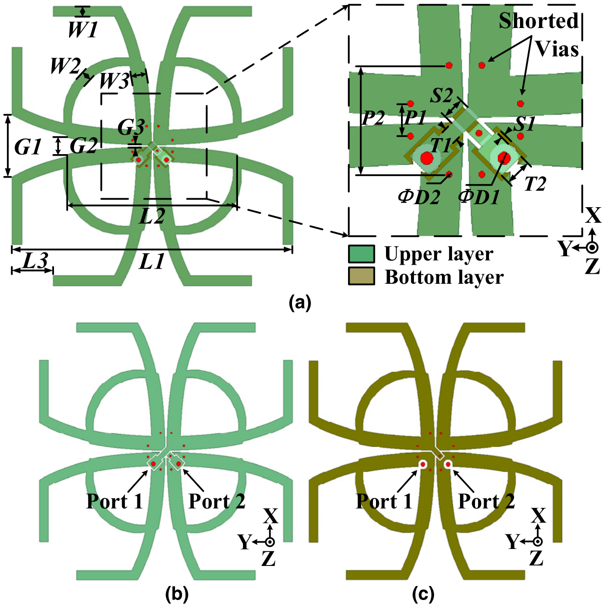

FIGURE 2. Detailed geometry of the proposed dipole antenna. (a) Geometry of the antenna. (b) Upper layer from top view. (c) Bottom layer from top view. ($L1 = 36.8$ mm, $L2 = 22$ mm, $L3 = 5.4$ mm, $W1 = 1.3$ mm, $W2 = 1.3$ mm, $W3 = 1.94$ mm, $G1 = 8.2$ mm, $G2 = 2.2$ mm, $G3 = 0.23$ mm, $S1 = 0.2$ mm, $S2 = 1.1$ mm, $T1 = 0.7$ mm, $T2 = 1.3$ mm, $P1 = 1.56$ mm, $P2 = 5.23$ mm, $D1 = 0.6$ mm, $D2 = 0.3$ mm, $k1 = 0.13$, and $k2 = 0.2$).

bandpass filters are placed under the crossed dipoles to reduce the minimum gain to −2.66 dBi in the notched band [13]. However, these aforesaid crossed dipole antennas all achieve notches by employing additional filtering circuits.

In this paper, a DBDP crossed dipole antenna is proposed to achieve a deep band-notch without extra circuit. Firstly, the original dipole antenna is presented by utilizing the modified feeding structure [14], [15] to realize wide-band or dual-band performance. Then, the band-notch (3.4-3.6 GHz) is achieved by introducing the C-shaped split ring resonators (SRRs) into the dipole arms. Compared with the original wideband antenna covering 2.4-5.8 GHz for VSWR < 2 in [15], the minimum gain in the notched band is suppressed from 8 dBi to −9 dBi, the antenna profile can be lowered from 19.5 mm to 16 mm, and the gain is improved from 6 dBi to 9.7 dBi in the higher band. As a result, the proposed DBDP antenna, working in 2.39-2.69 GHz and 4.98-6.36 GHz with isolation > 27 dB for VSWR < 2, can be used for MIMO WLAN applications with high isolation and high gain.

II. ANTENNA DESIGN

A. STRUCTURE OF ANTENNA

The overall structure of the proposed antenna is depicted in Fig. 1. It is composed of one substrate supported by four plastic posts, two coaxial cables and a metallic reflector. The crossed dipoles are printed on the upper and bottom layers of the substrate, and fed by two coaxial cables. The substrate is the Rogers-4350 with a permittivity of $\varepsilon_r = 3.66$, a length of $Ls = 37.5$ mm and a thickness of $Hs = 0.787$ mm. Beneath the substrate, a square metallic reflector is employed, with a distance of $H = 16$ mm to realize a unidirectional radiation pattern.

The detailed geometry of the crossed dipole antenna is shown in Fig. 2. As can be seen in Fig. 2(a), each arm of dipole antenna has a small internal ring and an external split ring. The arm of the antenna is designed in exponential shape. The exponential function can be expressed as $Y(x) = Ce^{kx} + B$. k is the constant coefficient for the exponential function, and $k1$ and $k2$ (here, $k1 = 0.13$ and $k2 = 0.2$ are selected) represent the coefficients of external and internal rings, respectively. Fig. 2(b) and (c) show the upper layer and lower layer from top view, respectively. The outer conductors of coaxial cables are connected directly to two pairs of dipoles on the lower layer, and the inner conductors are connected to another two pairs of dipoles on the upper layer. The arms on the upper and lower layers are connected to each other with eight shorted vias. As shown in the inset of Fig. 2(a), the arms are connected to the inner conductors through extra metallic strips on the upper layer. To avoid overlapping, part of one metallic strip is printed on the bottom layer of the substrate, and a metallic via is used to connect the upper and bottom parts of the metallic strip. Because four pairs of dipoles are structurally symmetric and the results of two ports are almost identical, all analyses are thus implemented on port 1 in the following content.

B. ANALYSIS OF ANTENNA DESIGN

The basic working principle of the crossed dipole antenna is that two pairs of dipoles are placed orthogonally to each other to achieve dual polarization. When the arms of two dipoles are designed close to each other, strong coupling between the driven and crossed elements introduces a second mode and the bandwidth of the crossed dipole antenna is broadened greatly [13], [14]. Moreover, the gap between the crossed arms is designed in gradual changing structure to further improve the impedance matching [14], [15]. In order to realize wide bandwidth, the exponential-shaped arms of the proposed dipole antenna are applied in this paper.

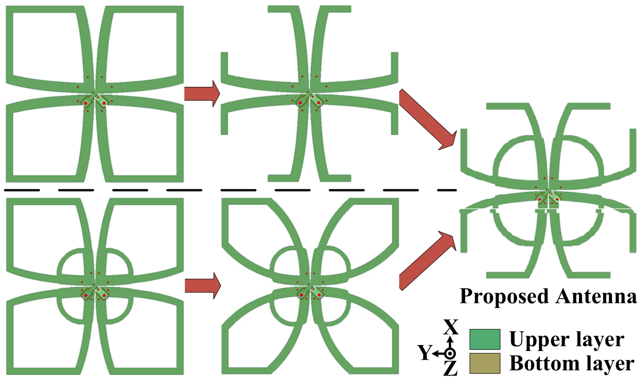

FIGURE 3. The evolution of the proposed antenna.

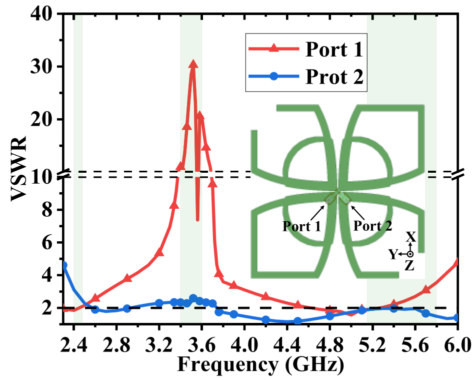

FIGURE 5. Simulated VSWRs of two ports with SRRs introducing to the parasitic pairs of dipoles.

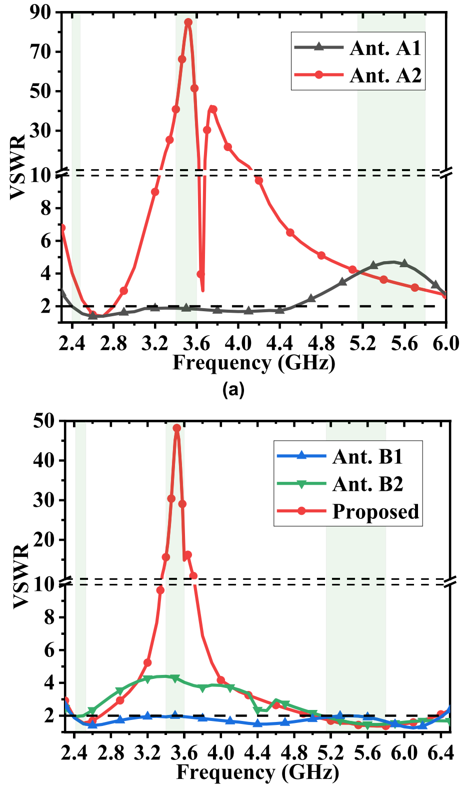

(a)

(b)

FIGURE 4. Simulated Results of (a) Ant. A1 and Ant. B1, and (b) Ant. B1, Ant. B2 and the proposed antenna.

Asmentioned above, the exponential function of the arm structure is expressed as $Y(x) = Ce^{kx} + B$. The smaller the coefficient k, the closer the exponential line is to a straight line.

In order to demonstrate the evolution of the proposed DBDP antenna, five types of crossed dipole antennas are designed and depicted in Fig 3 (Ant. A1, Ant. A2, Ant. B1, Ant. B2 and the proposed antenna). Ant. A1 is a wideband dipole antenna with two modes, and Ant. A2 is modified from Ant. A1 with band-notch. Ant. B1 is an ultra-wideband dipole antenna with three modes [15], and Ant. B2 is a dual-band dipole antenna modified from Ant. B1 with different *G1* and coefficient k.

The VSWR comparison between Ant. A1 and Ant. A2 is shown in Fig. 4(a). The bandwidth of Ant. A1 is 2.4-4.54 GHz (62%) for VSWR <2. Although a deep notch can be generated with C-shaped arms of Ant. A2, the impedance of all WLAN bands is mismatched. The VSWR comparison among Ant B1, Ant. B2 and the proposed antenna is presented in Fig. 4(b). Ant. B1 with double rings can realize the bandwidth of 2.38-6.42 GHz (91%). Ant. B2 with two working bands can covers WLAN bands, but the suppression for 3.4-3.6 GHz is not good enough. The proposed antenna can achieve a deep rejection and two operating bands covering WLAN 2.4-GHz and 5-GHz bands.

In order to investigate the working principle of the notched band, the SRRs are only introduced into one pair of dipoles with port 2, as shown in the inset of Fig. 5. The VSWRs of two ports are depicted in Fig. 5. It can be seen that port 1 achieves a notched band, while port 2 still has the wideband characteristic. That is, the notched band of port 1 is realized by the SRRs of the coupling parasitic dipole. Consequently, when SRRs are introduced into two pairs of dipoles, the notched bands can be achieved for two ports.

The surface current distribution is displayed in Fig. 6 to further explain the radiation mechanism of the proposed antenna. Since two layers of the crossed dipoles have the same current distributions, only the current distributions on the upper layer are displayed and analyzed. When port 1 is excited, the surface current distributions over a quarter period of the excitation phase of $\psi = 0, \pi/4$ and $\pi/2$ are presented at 2.4, 3.5 and 5.8 GHz. 2.4, 3.5 and 5.8 GHz are the lowest WLAN frequency, notched frequency, highest WLAN frequency, respectively. $\psi = 0$ and $\pi/2$ are two states in which the dipole current antinode has the minimum and maximum values, respectively. The red arrows represent the maximum surface currents on the proposed antenna.

At 2.4 GHz frequency, the maximum surface currents (red arrows) are all distributed on the driven dipole at three excitation phases of $\psi = 0, \pi/4$ and $\pi/2$. The current antinodes appear at the feed portion for three phase states. At 5.8 GHz, the maximum surface currents also occur at the driven dipole. The current antinodes appear at different locations for three

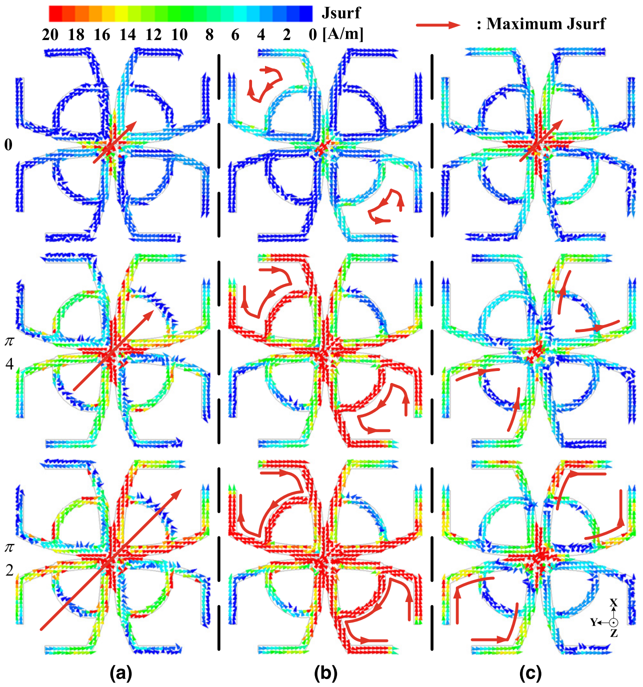

FIGURE 6. Surface current distributions on the upper layer of the proposed antenna over a quarter period of the excitation phase ψ at (a) 2.4 GHz, (b) 3.5 GHz and (c) 5.8 GHz.

phase states. At the notched frequency of 3.5 GHz, the maximum currents are distributed on the C-shaped arms of the coupling parasitic dipole. The currents on two arms of the parasitic dipole are in clockwise and counterclockwise directions. The results show that two working frequency bands are attributed to the radiation of the driven dipole, and the notched band are introduced by the C-shaped SRRs of the coupling parasitic dipole.

C. PARAMETERS OF ANTENNA DESIGN

Fig. 7(a)-(c) show the impacts of parameters $L2$, $L3$, and H on VSWR, respectively. As shown in Fig. 7(a), when $L2$ increases, the first working band and notched band move toward higher frequency, while the second working band moves toward lower frequency. Fig. 7(b) shows that when $L3$ becomes larger, the whole frequency band moves to higher frequency. According to Fig. 7(c), the impedance matching of two working frequency bands are improved as H increases. When $H = 16$ mm, the VSWR < 2 in two working bands, and when $H = 18$ mm, the impedance can be improved with VSWR < 1.5. Therefore, it can be concluded that the locations of two working bands and notched band can be controlled jointly by $L2$ and $L3$, and the impedance matching can be improved by increasing the value of H.

III. PERFORMANCE OF ANTENNA

The simulation analyses are performed by Ansys HFSS, and the measurements are implemented by the Agilent network analyzer (Agilent N5230A) and far-field measurement system (NSI 2000). The fabricated Ant. B1, Ant. B2 and

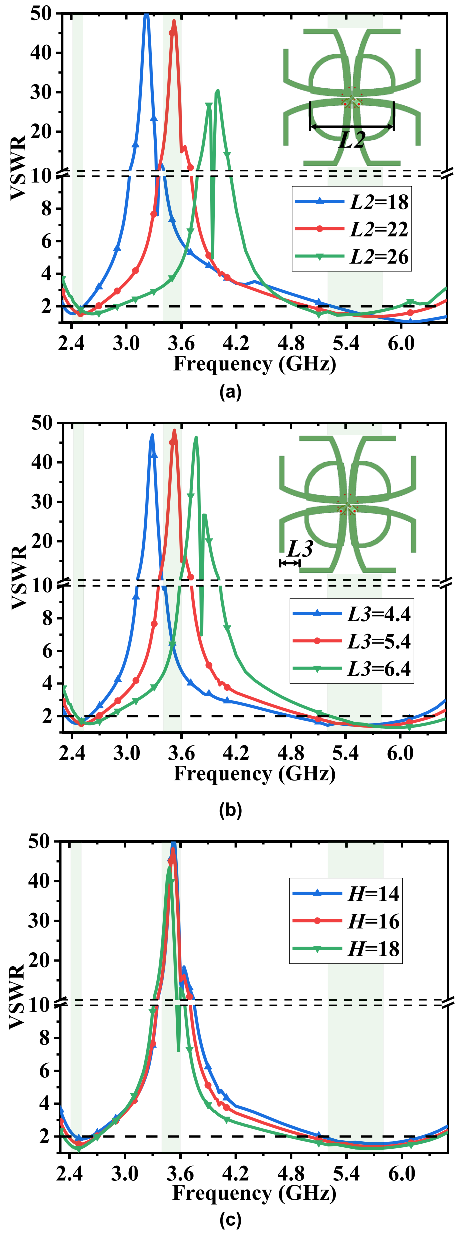

FIGURE 7. Impacts of (a) $L2$, (b) $L3$, and (c) H on VSWR.

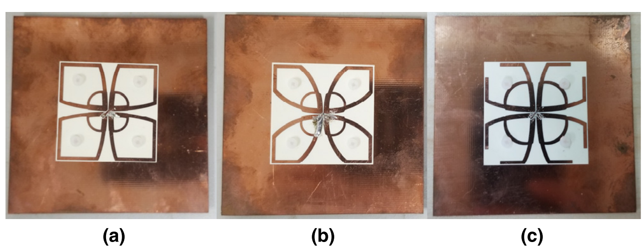

FIGURE 8. The fabrication of (a) Ant. B1, (b) Ant. B2 and (c) the proposed antenna.

the proposed antenna are shown in Fig. 8(a), (b) and (c), respectively.

The simulated and measured VSWRs of these three antennas are shown in Fig. 9(a). The measured bandwidth of Ant.

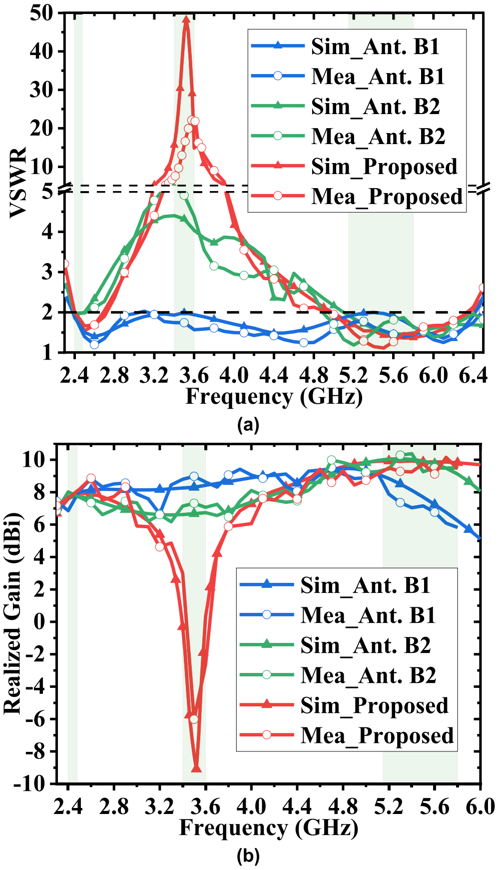

FIGURE 9. Simulated and measured (a) VSWRs and (b) realized gain of three antennas.

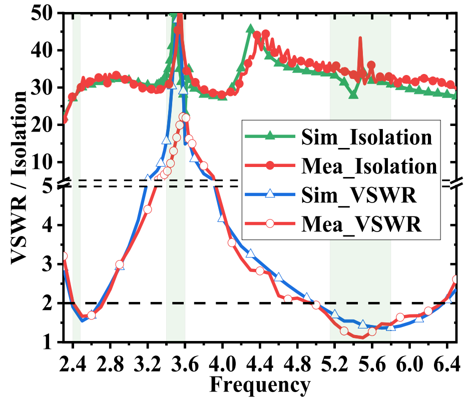

FIGURE 10. Simulated and measured VSWR and isolation.

TABLE 1. Comparison of different antennas.

Ref.	BW/GHz	Iso. /dB	Gain /dBi	Possible for WLAN	Band Notch	Extra circuit	Planar structure
[2]	2.34-2.6 & 4.87-5.52	22	7.2 7.3	YES	NO	-	NO
[3]	2.3-2.75 & 4.56-5.95	-	5.1 6	YES	NO	-	YES
[5]	2.40-2.49 & 3.39-3.69 & 4.80-5.91	20	7 7.5 9.5	YES	NO	-	YES
[10]	5.2-5.25 & 5.6-6.35	-	7 8	NO	YES	Without	NO
[11]	2.6-6 & 7.5-14.9	-	>5	YES	YES	With	YES
[13]	1.7-2.27 & 2.53-2.9	24	7.57	NO	YES	With	NO
This work	**2.4-2.65 & 5-6.4**	**27**	**7.85 9.7**	**YES**	**YES**	**Without**	**YES**

B1 is 2.4-6.38 GHz, and the two working bands of Ant. B2 are 2.4-2.5 GHz and 4.9-6.5 GHz for VSWR < 2. The measured results show that the proposed antenna has two operating bands of 2.4-2.7 GHz and 4.95-6.35 GHz with a deep band-notch for 3.4-3.6 GHz. The simulated and measured realized gain of three antennas are depicted in Fig. 9(b). Ant. B1 achieves wideband gain characteristic of 5.8-9.4 dBi and the gain decreases to 6 dBi in the WLAN 5-GHz bands. The gain of Ant. B2 is around 7.85 dBi in the 2.4-GHz band and over 9.2 dBi in the 5-GHz bands. The measured average gain of the proposed antenna is 7.85 dBi in the lower working band and 9.7 dBi in the higher working band. The minimum gain in the notched band is -6 dBi, which is 15 dB less than the measured gain of Ant. B1 at 3.5 GHz. It can be seen that by changing the constant coefficient of the exponential function and introducing the SRR, the realized gain of the higher band can be improved by suppressing the realized gain of the notched band. The measured results have a good agreement with the simulated ones. The deviation between the simulated and measured results is mainly caused by the fabrication and wideband measurement tolerance.

The simulated and measured isolation of the proposed antenna are shown in Fig. 10. The overlapped measured bandwidth of two ports covers the WLAN bands for VSWR < 2, and the isolation is better than 27 dB for the two working bands. The radiation patterns at the horizontal plane (YOZ plane) for 2.4, 5.2 and 5.8 GHz are presented in the Fig. 11(a), (b) and (c), respectively. The co-polarization patterns are stable and the measured cross-polarization is less than 25 dB.

The comparison among the proposed antenna and some reported works is shown in Table 1. These reference works are all DBDP antennas with unidirectional radiation patterns. Dipole antennas in [2] and [3] use parasitic elements to achieve dual working bands. However, antenna in [2] is complicated in structure and antenna in [3] has high profile and low gain. The crossed dipole antenna in [5] is designed for tri-band applications with no band-notch. The work [10] utilizes microstrip antenna to achieve band-notch without additional circuit, but the bandwidth of the antenna is not wide enough for 2.4/5 GHz WLAN applications. Although the Vivaldi antenna with wide bandwidth in [11] can realizes dual bands by introducing filtering circuit near the balun structure, it is high in profile and low in gain. The paper [13] needs to use extra feeding structure under the crossed dipole antenna to achieve a band-notch, and the bandwidth is unable to cover 2.4/5 GHz WLAN bands. It can be seen that the proposed antenna can achieve DBDP band-notched characteristics for WLAN applications with high gain and high isolation.

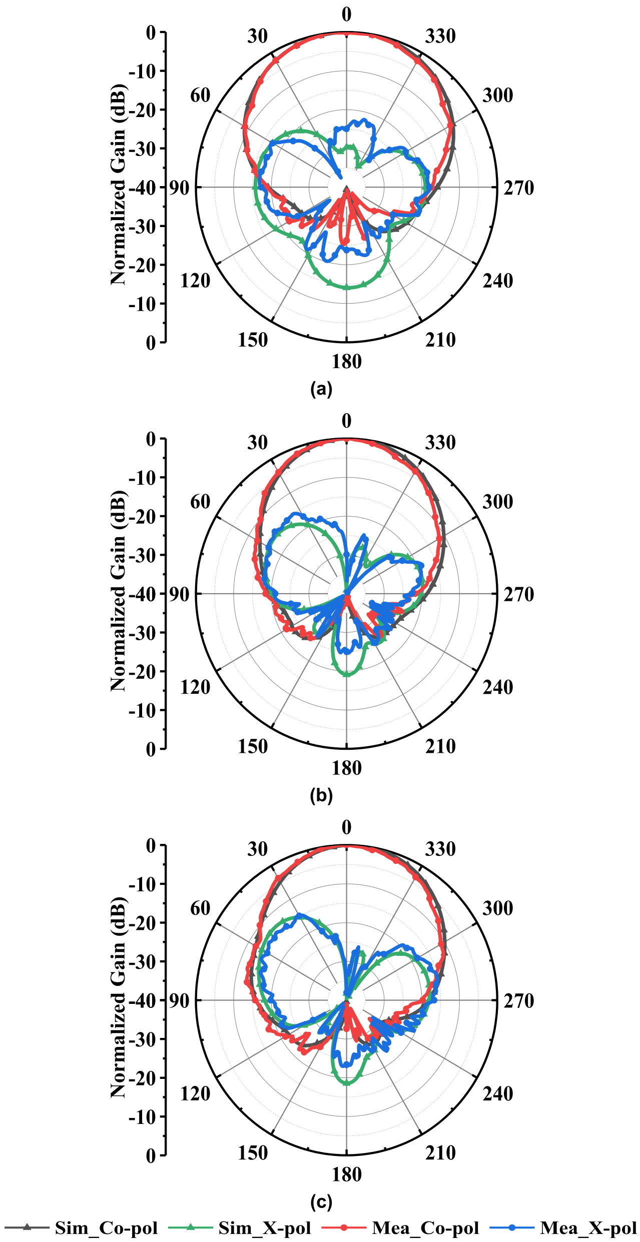

FIGURE 11. Simulated and measured radiation patterns at the horizontal plane for (a) 2.4 GHz, (b) 5.2 GHz, (c) 5.8 GHz.

Moreover, it is easy for fabrication with planar structure and no extra circuit.

IV. CONCLUSION

A DBDP crossed dipole antenna with band-notch is proposed for WLAN applications in this paper. The proposed antenna can realize two working bands (WLAN 2.4-GHz band and 5-GHz bands) and a notched band (3.4-3.6 GHz) with isolation > 27 dB. Without extra filtering circuit, the band-notch is achieved by modifying the arm of dipole into C-shaped split ring. Moreover, the proposed antenna can realize high gain of 7.85 dBi for the lower band and 9.7 dBi for the higher band. Because of the stable unidirectional radiation patterns and DBDP band-notched characteristics with high isolation and high gain, the proposed antenna can be an excellent candidate for wireless communication systems, such as the MIMO WLAN applications.

REFERENCES

[1] T.-W. Chiou and K.-L. Wong, "A compact dual-band dual-polarized patch antenna for 900/1800-MHz cellular systems," *IEEE Trans. Antennas Propag.*, vol. 51, no. 8, pp. 1936–1940, Aug. 2003.

[2] H. Zhai, K. Zhang, S. Yang, and D. Feng, "A low-profile dual-band dual-polarized antenna with an AMC surface for WLAN applications," *IEEE Antennas Wireless Propag. Lett.*, vol. 16, pp. 2692–2695, 2017.

[3] J. M. Steyn, J. Joubert, and J. W. Odendaal, "A polarization diverse antenna for dual-band WLAN applications," in *Proc. Eur. Microw. Conf. (EuMC)*, Rome, Italy, Sep./Oct. 2009, pp. 540–543.

[4] W. C. Zheng, L. Zhang, Q. X. Li, and Y. Leng, "Dual-band dual-polarized compact bowtie antenna array for anti-interference MIMO WLAN," *IEEE Trans. Antennas Propag.*, vol. 62, no. 1, pp. 237–246, Jan. 2014.

[5] Y. Pan, Y. Cui, C. L. Qi, and R. Li, "Evaluation of dual-polarised triple-band multi-beam MIMO antennas for WLAN/WiMAX applications," *IET Microw., Antennas Propag.*, vol. 11, no. 10, pp. 1469–1475, Aug. 2017.

[6] J. Deng, S. Hou, L. Zhao, and L. Guo, "A reconfigurable filtering antenna with integrated bandpass filters for UWB/WLAN applications," *IEEE Trans. Antennas Propag.*, vol. 66, no. 1, pp. 401–404, Jan. 2018.

[7] J. Deng, S. Hou, L. Zhao, and L. Guo, "Wideband-to-narrowband tunable monopole antenna with integrated bandpass filters for UWB/WLAN applications," *IEEE Antennas Wireless Propag. Lett.*, vol. 16, pp. 2734–2737, 2017.

[8] C.-X. Mao, S. Gao, Y. Wang, Q. Luo, and Q.-X. Chu, "A shared-aperture dual-band dual-polarized filtering-antenna-array with improved frequency response," *IEEE Trans. Antennas Propag.*, vol. 65, no. 4, pp. 1836–1844, Apr. 2017.

[9] C.-X. Mao, S. Gao, Y. Wang, Y. Liu, X.-X. Yang, Z.-Q. Cheng, and Y.-L. Geng, "Integrated dual-band filtering/duplexing antennas," *IEEE Access*, vol. 6, pp. 8403–8411, 2018.

[10] M. Xun, W. Yang, W. Feng, W. Che, and H. Jin, "Novel dual-polarized and closely dual-band filtering patch antenna array with good band-notched function," in *Proc. 6th Asia–Pacific Conf. Antennas Propag. (APCAP)*, Xi'an, China, Oct. 2017, pp. 1–3.

[11] H. Feng, F. Zhang, and H. Zhang, "A dual polarized vivaldi antenna with the notched band by feed line filter on conductive plane," in *Proc. Int. Conf. Microw. Millim. Wave Technol. (ICMMT)*, Chengdu, China, May 2018, pp. 1–3.

[12] Y. Liu, S. Wang, N. Li, J.-B. Wang, and J. Zhao, "A compact dual-band dual-polarized antenna with filtering structures for sub-6 GHz base station applications," *IEEE Antennas Wireless Propag. Lett.*, vol. 17, no. 10, pp. 1764–1768, Oct. 2018.

[13] H. Huang, Y. Liu, and S. Gong, "A broadband dual-polarized base station antenna with anti-interference capability," *IEEE Antennas Propag. Lett.*, vol. 16, pp. 613–616, 2017.

[14] Y. Zhang, D. Li, Y. Zhang, and Y. Fan, "Compact wideband dual-polarized antenna with high isolation using modified direct feeding structure for indoor beamforming array applications," *IEEE Access*, vol. 6, pp. 66396–66402, 2018.

[15] Y. Zhang, D. Li, Y. Zhang, K. Liu, and Y. Fan, "Ultra-wideband dual-polarized antenna with three resonant modes for 2G/3G/4G/5G communication systems," *IEEE Access*, vol. 7, pp. 43214–43221, 2019.

YAOHUI ZHANG received the B.S. degree in electromagnetic wave propagation and antenna from the University of Electronic Science and Technology of China (UESTC), Chengdu, China, in 2014, where he is currently pursuing the Ph.D. degree in electromagnetic field and microwave technology.

His research interests include compact and wideband antennas, and microwave filter.

YONGHONG ZHANG received the B.S., M.S., and Ph.D. degrees from the University of Electronic Science and Technology of China (UESTC), Chengdu, China, in 1992, 1995, and 2001, respectively.

From 1995 to 2002, he was a Lecturer with UESTC. From 2002 to 2004, he was a Postdoctoral Fellow with the Department of Electronic Engineering, Tsinghua University, Beijing, China. Since 2004, he has been with UESTC, where he is currently a Full Professor with the School of Electronic Science and Engineering. His research interest includes microwave and millimeter wave technology and applications. He is also a Senior Member of the Chinese Institute of Electronics.

DAOTONG LI (S'15–M'16) received the Ph.D. degree in electromagnetic field and microwave technology from the University of Electronic Science and Technology of China (UESTC), Chengdu, China, in 2016.

Since 2015, he has been a Visiting Researcher with the Department of Electrical and Computer Engineering, University of Illinois at Urbana–Champaign, Urbana, IL, USA, with financial support from the China Scholarship Council. He is currently with the Center of Aerocraft TT&C and Communication, Chongqing University, Chongqing. He has authored or coauthored over 50 peer-reviewed journals or conference papers. His current research interests include RF, microwave and millimeter-wave technology and applications, antennas, devices, circuits and systems, and passive and active (sub-) millimeter-wave imaging and radiometer.

Dr. Li was a recipient of the UESTC Outstanding Graduate Awards by the Sichuan province and UESTC, in 2016. He was also a recipient of the National Graduate Student Scholarship from the Ministry of Education, China, and the Tang Lixin Scholarship. Since 2014, he has been serving as a Reviewer for some international journals. He is serving as a Reviewer for several IEEE and IET journals, and many international conferences as a TPC Member, a Session Organizer, and the Session Chair.

KUNNING LIU was born in Sichuan, China, in 1992. He received the B.S. degree in electromagnetic wave propagation and antenna from the University of Electronic Science and Technology of China (UESTC), Chengdu, in 2015, where he is currently pursuing the Ph.D. degree in electromagnetic, under the supervision of Prof. S. Yang.

His current research interests include lens antennas, stratified media, and meta-material.

YONG FAN received the B.E. degree from the Nanjing University of Science and Technology, Jiangsu, China, in 1985, and the M.S. degree from the University of Electronic Science and Technology of China (UESTC), Chengdu, China, in 1992.

He is currently a Full Professor with the School of Electronic Science and Engineering, UESTC. He is also the IEEE member, a Senior Member of the Chinese Institute of Electronics. He has authored or coauthored more than 200 papers. His current research interests include electromagnetic theory, millimeter-wave and terahertz circuits, and communication technology.